

Fractal stabilization of Wannier-Stark resonances

M. GLÜCK¹, A. R. KOLOVSKY^{1,2} and H. J. KORSCH¹

¹ *Fachbereich Physik, Universität Kaiserslautern, D-67653 Kaiserslautern, Germany*

² *Kirensky Institute of Physics, 660036 Krasnoyarsk, Russia*

(received ; accepted in final form)

PACS. 03.65.-w- Quantum mechanics.

PACS. 05.45.-a- Chaotic and nonlinear dynamical systems.

PACS. 73.20.Dx- Electron states in low-dimensional structures.

Abstract. – The quasienergy spectrum of a Bloch electron affected by dc-ac fields is known to have a fractal structure as function of the so-called electric matching ratio, which is the ratio of the ac field frequency and the Bloch frequency. This paper studies a manifestation of the fractal nature of the spectrum in the system “atom in a standing laser wave”, which is a quantum optical realization of a Bloch electron. It is shown that for an appropriate choice of the system parameters the atomic survival probability (a quantity measured in laboratory experiments) also develops a fractal structure as a function of the electric matching ratio. Numerical simulations under classically chaotic scattering conditions show good agreement with theoretical predictions based on random matrix theory.

1. – In this letter we study the spectral and dynamical properties of a Bloch particle affected by static and time-periodic forces:

$$\hat{H} = \hat{p}^2/2 + \cos x + Fx + F_\omega \cos(\omega t) x, \quad \hat{p} = -\hbar' d/dx, \quad (1)$$

where \hbar' is the scaled Planck constant (see below). Originally this problem was formulated for a Bloch electron in dc-ac electric fields $\hat{H} = \hat{p}^2/2m + V(x) + e[E + E_\omega \cos(\omega t)]x$, $V(x+a) = V(x)$ [1] and attracted much attention because of the similarity with the Hofstadter problem [2]. Indeed, the energy spectrum of a Bloch electron in a 2D lattice under the action of a constant magnetic field B depends on the magnetic matching ratio $\beta = h/eBa^2$ (a is the lattice constant) and has a fractal structure as function of this parameter. Analogously, the quasienergy spectrum of system (1) depends on the electric matching ratio

$$\alpha = \frac{\omega}{\omega_B}, \quad \omega_B = \frac{2\pi F}{\hbar'}, \quad (2)$$

where ω_B is the Bloch frequency, which is $\omega_B = eEa/\hbar$ in the case of a crystal electron. For rational ratios $\alpha = r/q$ the quasienergy spectrum has a band structure; it is discrete, however, for irrational values of α [1]. Numerically the quasienergy spectrum of the system (1) was studied in ref. [3] by using the tight-binding approximation. It was shown that for $\alpha = r/q$

the quasienergy bands are arranged in a structure resembling the famous Hofstadter butterfly (see Fig. 1 in Ref. [3]). It should be pointed out, however, that the results of paper [3] only partially describe the spectrum of the system (1) because the tight-binding approximation neglects the decay of the quasienergy states. The actual quasienergy spectrum is complex, where the imaginary part of the spectrum defines the lifetimes of the metastable quasienergy states.

Because of the extremely small lattice period in crystals, the fractal structure of the quasienergy spectrum has never been observed in solid state systems. However, a signature of it was recently found in an experiment with cold atoms in an optical lattice [4]. The latter system models the solid state Hamiltonian (1), where the neutral atoms moving in the optical potential $V(x)$ (k_L is the laser wave vector) take over the role of the crystal electrons. The effect of the electric fields can be mimicked, for example, by the inertial force induced by accelerating the experimental setup as a whole. (In practice, however, the acceleration was obtained by an appropriate chirping of the laser frequency.) The system “atom in a standing wave” has an essentially larger lattice period than the solid state system and is, in addition, free of relaxation processes due to scattering by impurities and the Coulomb interaction. These features of the system were utilized earlier in ref. [5] to observe experimentally the Wannier-Stark ladder of resonances. The main modification of the experiment [4] in comparison with the experiment [5] is that a strong periodic driving with frequency $\omega = (r/q)\omega_B$ was imposed. (Only the cases $r/q = 1/2$ and $r/q = 1/3$ were reported.) Then the atomic survival probability as a function of the frequency of the probe signal shows additional anti-peaks (see fig. 3 in ref. [4]), which were interpreted as an indication of the fractal structure of the spectrum. We note that the width of these anti-peaks is given by the width (*i.e.* the inverse lifetime) of the first excited Wannier-Stark resonances. This imposes a fundamental restriction on the resolution and it seems impossible to resolve matching ratios $\alpha = \omega/\omega_B$ for α different from lowest rational numbers.

2. – The discussed papers [3, 4] study the system in the deep quantum region. In the present paper we discuss the manifestation of the fractal structure of the quasienergy spectrum in the semiclassical region of the system parameters. We shall show that in this region the fractal nature of the spectrum can be observed without using a probe signal and the electric matching ratio can be resolved with any desired accuracy.

The characteristic measure of the systems “classicality” is the scaled Planck constant \hbar' entering the momentum operator in the Hamiltonian (1). Referring to the system “atom in a standing wave” the scaled Planck constant is given by

$$\hbar' = \left(\frac{8\hbar\omega_{rec}}{V_0} \right)^{1/2}, \quad (3)$$

where $\omega_{rec} = \hbar k^2/2m$ is the atomic recoil frequency and V_0 is the depth of the optical potential $V(x) = V_0 \cos^2(k_L x)$. In the experiments [4] and [5] the value of the scaled Planck constant was $\hbar' \approx 1.5$ and 1.6, respectively. In our numerical studies we use $\hbar' = 0.25$. Since the amplitude V_0 of the optical potential is proportional to the square of the laser field amplitude, this implies a larger intensity of the laser.

We simulate the wave packet dynamics of the system (1) by numerical solution of the time-dependent Schrödinger equation in the momentum representation using parameters $\hbar' = 0.25$, $\omega = 10/6$, $F_\omega = 4.16$ with values of the static field F in the interval $0.030 \leq F \leq 0.083$. Then the survival probability

$$P(t) = \int_{|p| < p_0} |\psi(p, t)|^2 dp, \quad (4)$$

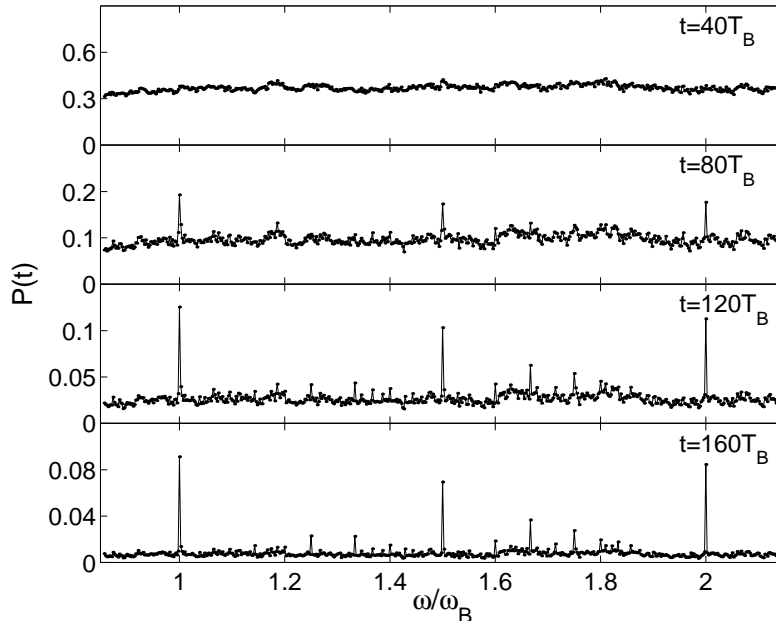


Fig. 1. – Time evolution of the atomic survival probability $P(t)$ calculated for rational values of the electric matching ratio $\omega/\omega_B = r/q$, $q \leq 420$ (see text). With increasing time $t = 40T_B, \dots, t = 160T_B$ the survival probability develops pronounced peaks at rationals with small denominators. The system parameters are $\hbar' = 0.25$, $\omega = 10/6$, $F_\omega/\omega^2 = 3/2$, and $0.031 < F < 0.077$.

is calculated. The initial state is the localized Wannier state, which for the cosine potential practically coincides with a minimal uncertainty wave packet centered at $x = \pi$. The motivation for the chosen value of $p_0 = 6$, which is much larger than the region of support of the initial wave packet, is given in sec. 3 below. This numerical simulation models the experimental situation of ref. [4] with the modification that there is no probe signal but the amplitude F of the static force is varied.

The result for the survival probability as a function of F — or, equivalently, as a function of the matching ratio $\alpha = \omega/\omega_B$ — is shown in fig. 1 and 2(a), which is the central result of the paper. The dots in fig. 1 mark the survival probability $P(t)$ calculated for increasing values of the observation time $t = 40T_B, \dots, t = 160T_B$. The values of static force F are chosen for rational values of the electric matching ratios $\omega/\omega_B = r/q$ with $q \leq 420$. (Explicitly, we considered for q all divisors of $2^2 \cdot 3 \cdot 5 \cdot 7 = 420$ and all coprime r -values in the interval $6/7 \leq r/q \leq 15/7$.) To guide the eyes, the dots are connected by a solid line. The actual width of the peaks, which is inversely proportional to the observation time, is smaller in fig. 2(a), which shows a more fully developed distribution for a longer time $t = 200T_B$. It is seen in fig. 2(a) that there are pronounced peaks above an almost constant background which appear at low order resonances between the driving frequency and the Bloch frequency. The seven largest peaks in the figure correspond (from left to right) to $r/q = 1, 5/4, 4/3, 3/2, 5/3, 7/4$, and $r/q = 2$, and the observed peak-heights fall off rapidly with increasing denominator q . As illustrated by fig. 1, this peak structure develops gradually in time, starting from $P(0) = 1$ at time zero and originates from the different long-time behavior of the survival probabilities. We

find exponential decay in time for irrational values of ω/ω_B and algebraic decay for rational ones [6]. Thus the survival probability as a function of F reflects the fractal nature of the spectrum in the long-time regime. Moreover, there is no fundamental resolution constraint and an arbitrary number of peaks can be resolved by increasing the observation time. We also note that instead of varying the static force one can vary the frequency ω of the driving force. In this case, having in mind a laboratory experiment, it looks reasonable to use the gravitational force as the static force [7].

3. – The key point of the conducted numerical experiment is that the amplitude F_ω and the frequency ω of the driving force are chosen such as to insure chaotic dynamics of the system in the classical limit. We furthermore choose p_0 in (4) to be larger than the boundary between the regular and the chaotic component of the classical phase space (see fig. 1(b) in ref. [8]). Then the classical survival probability decays exponentially [8]

$$P_{cl}(t) = \exp(-\nu t) , \quad (5)$$

where the decay coefficient ν , the inverse classical lifetime, is determined by the classical Lyapunov exponent and the fractal dimension of the chaotic repeller. We computed the classical decay rate numerically and determined the F -dependence of the classical decay rate as $\nu \approx 0.15 F$ in the parameter region considered here. It should be noted that the exponential decay of the classical probability cannot be considered as an universal law. In some systems it is a transient phenomenon and changes to an algebraic decay caused by long-lived trajectories sticking near stability islands [9, 10]. However, this is not the case for system (1) and no sign of an algebraic decay of the classical probability was detected (at least until time $t = 200T_b$, which was the maximal time in our numerical simulation).

Because we measure the observation time t in units of the Bloch period $T_B = \hbar'/F$, the F dependence in Eq. (5) cancels and the classical survival probability is practically constant. The quantum results follow closely the classical exponential decay (5) for irrational values of the matching ratio ω/ω_B providing the flat background of the quantum results shown in fig. 2. The peaks above the classical plateau for resonant driving, *i.e.* rational values of the matching ratio $\alpha = \omega/\omega_B$ are a quantum “stabilization”-phenomenon, which can be understood as follows.

It was shown in ref. [11] that the eigenvalue problem for the quasienergies of the system (1) for $\alpha = r/q$ can be mapped onto an effective scattering problem with q open channels. When the matching ratio α is an irrational number, the number of channel is infinite and the system follows the classical dynamics provided the condition $\hbar' \ll 1$ is satisfied. When the matching ratio is a rational number, however, the number of decay channels is finite and the quantum system (independent of the value of \hbar') is essentially more stable than the classical one [8]. In this case the behavior of the survival probability $P(t)$ differs from the exponential decay (5) and is determined by the distribution of the imaginary parts of the quasienergies, *i.e.* the distribution of the resonance widths.

In the case of chaotic classical dynamics an analytic expression for the resonance statistics is supplied by (non-hermitian) random matrix theory (RMT) [12, 13]. The validity of RMT for system (1) was checked numerically in ref. [11, 6] and a satisfactory correspondence was noticed. Converting the result of RMT from energy to time domain shows that the decay of the probability follows asymptotically an inverse power law [14]

$$P(t) \approx (\Gamma_W t / q \hbar')^q , \quad t \gg t^* \approx q \hbar' / \Gamma_W , \quad (6)$$

where Γ_W is the Weisskopf width, which is a free parameter in the abstract RMT. Identifying the parameter Γ_W / \hbar' with the classical decay coefficient ν , eq. (5) and eq. (6) can be combined

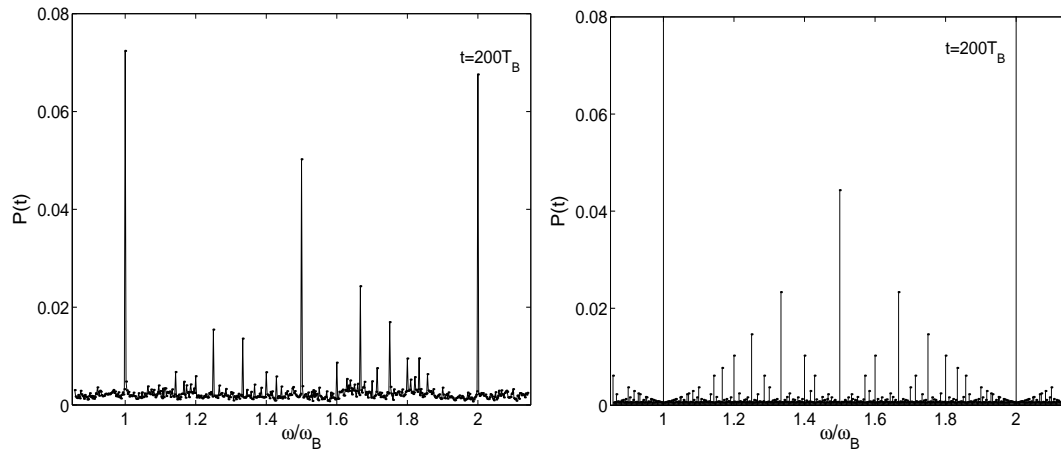


Fig. 2. – (a) Atomic survival probability $P(t)$ as shown in fig. 1, however for a longer time $t = 200 T_B$, where the fractal structure is much more clearly developed. To guide the eyes the dots are connected by a solid line but the actual width of the peaks, which is inversely proportional to the observation time, is smaller. (b) Survival probability $P(t) = (1 + \nu t/q)^{-q}$ (eq. (7)) derived from random matrix theory for $t = 200 T_B$. The value of the classical decay rate is $\nu = 0.15 F$.

in the single equation

$$P(t) = \left(1 + \frac{\nu t}{q}\right)^{-q}, \quad (7)$$

which has the correct short- and long-time asymptotic and provides a first crude approximation to the more elaborate RMT result [14].

Figure 2(b) shows the values of the function (7) for $t = 200 T_B$ and the same values of the matching ratio α as in fig. 2(a) where we use a slightly different graphic presentation of $P(t)$ to stress that the function (7) is a discontinuous function of α for any t . In contrast, the atomic survival probability shown in fig. 2(a) is a continuous function of F where its fractal structure develops gradually as $t \rightarrow \infty$. In fact, the probabilities (4) calculated for two close rational numbers α_1 and α_2 follow each other during a finite “correspondence” time. (For instance, for $\alpha_1 = 1$ and $\alpha_2 = 999/1000$ the correspondence time is found to be about $50 T_B$.) Thus it takes some time to distinguish two close rationals, although they may have very different denominators and, therefore, very different asymptotics (6). With this remark reserved, a nice structural (and even semiquantitative) correspondence is noticed. In addition, it seems worthwhile to note that also the pronounced quantum resonance peaks, *i.e.* the quantum algebraic decay $P(t) \approx (\nu t/q)^{-q}$ predicted by RMT, is mainly determined by the purely classical ν -coefficient due to classically chaotic scattering dynamics.

4. – We have analyzed the system (1) in context with recent experiments studying the dynamics of cold atoms in a standing laser wave [4]. It is shown that in the semiclassical region of the system parameters the atomic survival probability as a function of the static force (or, alternatively, of the driving frequency) shows a fractal structure. This fractal structure is actually related to the fractal nature of the quasienergy spectrum determined by the degree of rationality of the electric matching ratio (2). In fact, when a rational sequence

of $\alpha = r/q$ converges to some irrational value, the quasienergy bands progressively split into sub-bands. This process is accompanied by loss of stability of the quasienergy states and shows up, finally, in the complicated (fractal) structure of the atomic survival probabilities which can be measured in laboratory experiments.

Finally, we would like to distinguish the fractal structure of the survival probability discussed above from the fractal structure of the survival probability studied in papers [15, 16, 17]. The latter appears as a quantum manifestation of the hierarchical island structure of classical phase space in a system with an algebraic decay of the classical probability. The origin of the former phenomenon, however, is the fluctuating number of the decay channels depending on the value of the electric matching ratio (2), which is the control parameter of the system (1).

This work has been supported by the Deutsche Forschungsgemeinschaft (SPP 470 'Zeitabhängige Phänomene und Methoden in Quantensystemen der Physik und Chemie').

REFERENCES

- [1] ZHAO X.-G. and NIU Q., *Phys. Lett. A*, **191** (1994) 181.
- [2] HOFSTADTER D. R., *Phys. Rev. B*, **14** (1976) 2239.
- [3] ZHAO X.-G., JAHNKE R. and NIU Q., *Phys. Lett. A*, **202** (1995) 295.
- [4] MADISON K. W., FISHER M. C. and RAIZEN M. G., *Phys. Rev. A*, **60** (1999) R1767.
- [5] WILKINSON S. R., BHARUCHA C. F., MADISON K. W., NIU Q. and RAIZEN M. G., *Phys. Rev. Lett.*, **76** (1996) 4512.
- [6] GLÜCK M., KOLOVSKY A. R. and KORSCH H. J., *Physica E*, submitted.
- [7] ANDERSON B. P. and KASEVICH M. A., *Science*, **282** (1998) 1686.
- [8] GLÜCK M., KOLOVSKY A. R. and KORSCH H. J., *Phys. Lett. A*, **249** (1998) 483.
- [9] KLAFTER J., SHLESINGER M. F. and ZUMOFEN G., *Phys. Today, Feb.*, (1996) 33.
- [10] CHIRIKOV. B. V and SHEPELYANSKY D. L., *Phys. Rev. Lett.*, **82** (1999) 528.
- [11] GLÜCK M., KOLOVSKY A. R. and KORSCH H. J., *Phys. Rev. E*, **60** (1999) 247.
- [12] FYODOROV Y. V. and SOMMERS H.-J., *J. Math. Phys.*, **38** (1997) 1918.
- [13] ZYCKOWSKI K. and SOMMERS H.-J., *J. Phys. A: Math. Gen.*, **33** (2000) 2045.
- [14] SAVIN D. V. and SOKOLOV V. V., *Phys. Rev. E*, **56** (1997) R4911.
- [15] KETZMERICK R., *Phys. Rev. B*, **54** (1996) 10841.
- [16] CASATI G., GUARNERI I. and MASPERO G., *Phys. Rev. Lett.*, **84** (2000) 63.
- [17] HUCKESTEIN B., KETZMERICK R. and LEWENKOPF C. H., *preprint: cond/mat/9908090*, (1999).